

# MICROBUNCHING INSTABILITY MODELING IN THE SPARX CONFIGURATIONS

C. Vaccarezza, M. Ferrario, A. Marinelli INFN-LNF, Frascati, Italy  
M. Migliorati, Rome University « La Sapienza », Rome, Italy

## Abstract

The modeling of the microbunching instability has been carried out for the SPARX FEL accelerator, two configurations have been considered and compared: hybrid compression scheme (velocity bunching plus magnetic compressor) and purely magnetic. The effectiveness of a lattice tuning together with the use of a laser heater has been exploited to reduce the instability drawbacks on the electron beam quality. Analytical predictions and start to end simulation results are reported in this paper.

## INTRODUCTION

SPARX is a FEL project meant to provide a radiation wavelength in the range of  $\lambda_r = 40 \div 10$  nm,  $\lambda_r = 15 \div 3$  nm,  $\lambda_r = 4 \div 0.6$  nm, at 0.8-1.5-2.4 GeV respectively [1]. Two phases of construction are foreseen: the first with a maximum energy of 1.5 GeV and the second one up to 2.4 GeV. The 1.5 GeV accelerator has been considered in this paper to model the microbunching instability effect, comparing the two possible schemes of electron bunch compression: the “hybrid” one, velocity bunching in the photoinjector plus a magnetic chicane (BC2) at  $E \approx 500$  MeV, and the one based on a double magnetic compression at  $E \approx 300$  MeV (BC1) and at  $E \approx 500$  MeV (BC2). Starting from a theoretical approach of the microbunching instability effect in the coasting beam approximation [2,3], the two gain curves have been calculated looking for “tunability” margins of the accelerator lattice to limit the obtained gain peak value or to “move” it along the starting modulation wavelength axis to avoid destructive cooperation between the compression stages. The insertion of a laser heater chicane has also been studied for the two accelerator configurations and the simulation results are here reported.

Table 1: Electron Beam Parameter List

Energy	E (GeV)	1.5	2.4
Current	$I_{pk}$ (kA)	1	2.5
Norm. transverse emittance (slice)	$\epsilon_{nx}$ ( $\mu$ rad)	1	1
RMS energy spread (slice)	$\sigma_\delta$ (%)	<0.03	<0.02
Radiation wavelength	$\lambda_r$ ( $\mu$ m)	$13 \div 3$	$4 \div 0.6$

## THE 1.5 GEV SPARX LAYOUT

In Fig 1 the SPARX accelerator layout is shown. To reach the SASE saturation in reasonable length undulators a peak current  $I_{pk} \approx 1 \div 2.5$  kA is needed at the 1.5-2.4 GeV respectively. The required final beam energy spread is 0.1% (<0.03 % for the slice) in both cases and the nominal machine is designed to operate at a repetition rate of 100 Hz. The main parameter list is reported in Table 1 where the nominal beam energy, peak current, rms normalized emittance  $\epsilon_{nx}$ , rms energy spread  $\sigma_\delta$  and correspondent radiation wavelength are indicated. The SPARC photoinjector [4] provides the electron beam with energy  $\approx 150$  MeV, the 1.5 GeV accelerator section ends with the Linac3 and the electron beam is delivered to the first undulator U1, through the DL-1 transfer line, a four-dipole dogleg with an overall  $R_{56} < 1$  mm. The lattice from the photoinjector exit up to the DL1 end has been considered for this first modeling of the microbunching instability effect for the SPARX FEL: two bunch compressor chicanes are present, BC1 and BC2, at  $\approx 300$  MeV and  $500 \approx$  MeV respectively. A laser heater chicane is located at the exit of the photoinjector and a X-band cavity for the linearization of the beam longitudinal phase space is foreseen upstream the BC1 magnetic compressor. All the three Linac1-2-3 are equipped with three S-band, 3 m long, accelerating sections, with an accelerating gradient of  $E_{acc} \approx 23$  MV/m.

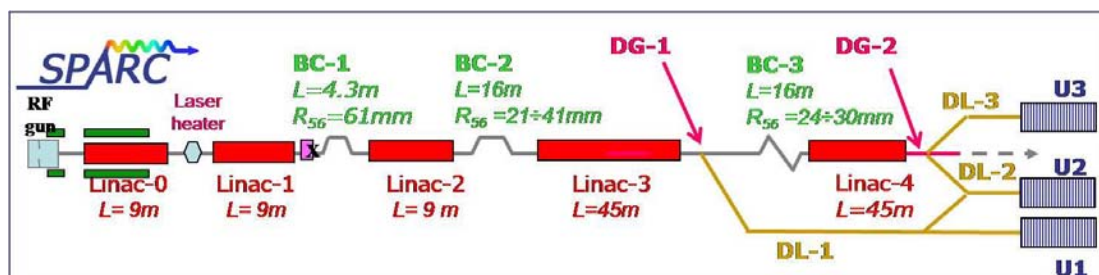


Figure 1: The SPARX Accelerator layout

## MICROBUNCHING INSTABILITY GAIN CURVE

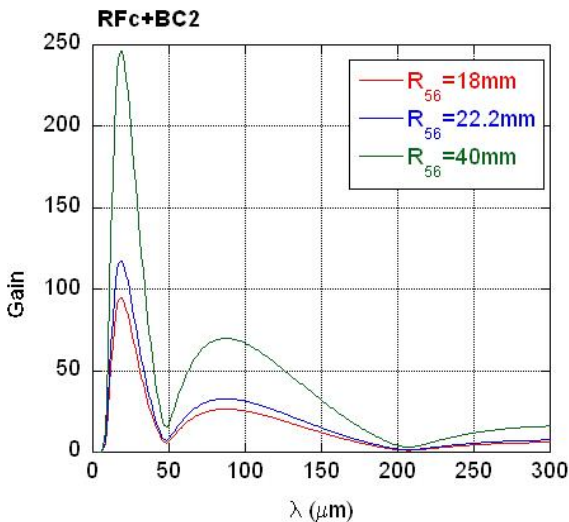
In the coasting beam approximation two expressions of the microbunching instability gain curve have been taken into account for RF compression and magnetic compression respectively: the first one is written as\* [2]:

$$G_1 = \frac{I_0}{I_A} \frac{4\pi Z_{LSC} S}{Z_0} (|M_{12}| C k) \exp\left(-\frac{(M_{12} C k_0 \sigma_{\delta u})^2}{2}\right) \quad (1)$$

where  $I_0$  is the uncompressed beam current,  $I_A$  the Alfven current,  $Z_{LSC}$  the longitudinal space charge impedance [3] for unit length averaged on the beam radius,  $Z_0$  the vacuum impedance,  $\sigma_{\delta u}$  is uncorrelated energy spread,  $k_0$  the initial modulation wave number,  $S$  the plasma oscillation term, and  $C$  the compression factor. For the microbunching gain of a magnetic compressor due to its upstream LSC impedance we have instead [3]:

$$G_2 \cong \frac{I_0}{I_A} \left| k_f R_{56} \int_0^L ds \frac{4\pi Z_{LSC}(k_0; s)}{Z_0} \right| \times \exp\left(-\frac{1}{2} k_f^2 R_{56}^2 \sigma_{\delta u}^2\right) \quad (2)$$

Where  $k_f$  is the compressed modulated wave number and  $R_{56}$  is the momentum compaction. In Fig. 2 the combination of G1 and G2, velocity bunching plus magnetic compression in BC2, is shown for different values of BC2 momentum compaction  $R_{56}$  while keeping constant the compression factor in the photoinjector and the final rms bunch length at the end of the final compression. In Fig. 3 the value of expression (2) has been reported as obtained for the BC1+BC2 configuration



\* Ifigure 2: The microbunching gain curve for the aPSPARX hybrid compression scheme velocity bunching plus magnetic chicane BC2

starting from an uncorrelated energy spread of  $\sigma_r \approx \pm 3\text{keV}$ , and varying the two momentum compaction factors to reduce the gain peak value. Just looking at the two curves the purely magnetic compression shows again peak value significantly higher than in the hybrid compression case at modulation wavelengths lower than  $\lambda_0 < 20\mu\text{m}$ . In table 2 the simulation results are reported referring to the nominal values and the “tuned” ones: 1.5 M particles for 1nC electron beam obtained with the PARMELA code through the SPARC photoinjector are tracked through the 1.5 GeV accelerator channel, up to the DL-1 dogleg end, by means of the ELEGANT code. The starting modulation wavelengths are:  $\lambda_0 = 40\mu\text{m}$ , with 8% ripple amplitude, and  $\lambda_0 = 250\mu\text{m}$  with 5% ripple amplitude. In all the configurations the rms final bunch length was kept  $\sigma_s \approx 110\mu\text{m}$  for the “hybrid” scheme and  $\sigma_s \approx 90\mu\text{m}$  for the purely magnetic compression, for a final peak current  $I_{\text{peak}} \approx 1\text{kA}$ .

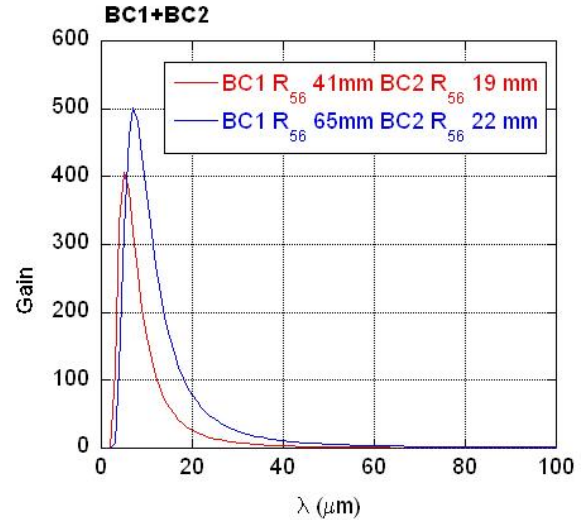


Figure 3: The microbunching gain curve for the SPARX purely magnetic scheme: BC1+BC2 compressors.

Table 2: Simulations results for the two SPARX configurations.

Velocity Bunching + BC2				
BC2- $R_{56}$ (mm)	nominal: 22.0		“tuned”: 18.8	
$\lambda_0$ ( $\mu\text{m}$ )	40	250	40	250
$\epsilon_{n,x,y}$ slice ( $\mu\text{m}$ )	1.	1.	1.	1.
$\sigma_{\delta}$ slice (%)	0.2	0.2	<0.02	<0.05
$\lambda_f$ ( $\mu\text{m}$ )	5.2	4.2	7.2	19.
$A_f$ (%)	34.5	43.4	3.2	26.
BC1+BC2				
BC1/BC2 $R_{56}$ (mm)	nominal: 65.0/22.0		“tuned”: 41.0/19.0	
$\lambda_0$ ( $\mu\text{m}$ )	40	250	40	250
$\epsilon_{n,x,y}$ slice ( $\mu\text{m}$ )	1.	1.	1.	1.
$\sigma_{\delta}$ slice (%)	0.2	0.1	<0.02	<0.02
$\lambda_f$ ( $\mu\text{m}$ )	4.4	3.2	8.1	32.
$A_f$ (mm)	32.3	40.9	3.9	26.8

In Fig. 4-5-6 the energy spread slice analysis are reported for the two compression schemes and the two considered starting modulated wavelengths, 40-250  $\mu\text{m}$ . In Fig 6 it is evident the residual peak in the energy spread for the “hybrid” configuration; for this reason a suitable laser heater parameter list has been set up as reported in Table 3 and the simulation results are shown in Fig.7. With the help of the laser heater is possible to reduce the residual structure in the energy spread, for the hybrid scheme with  $\lambda_0=250 \mu\text{m}$ , even though the simulation may be partially affected by the numerical noise due to the limited statistics of 1.5M particles.

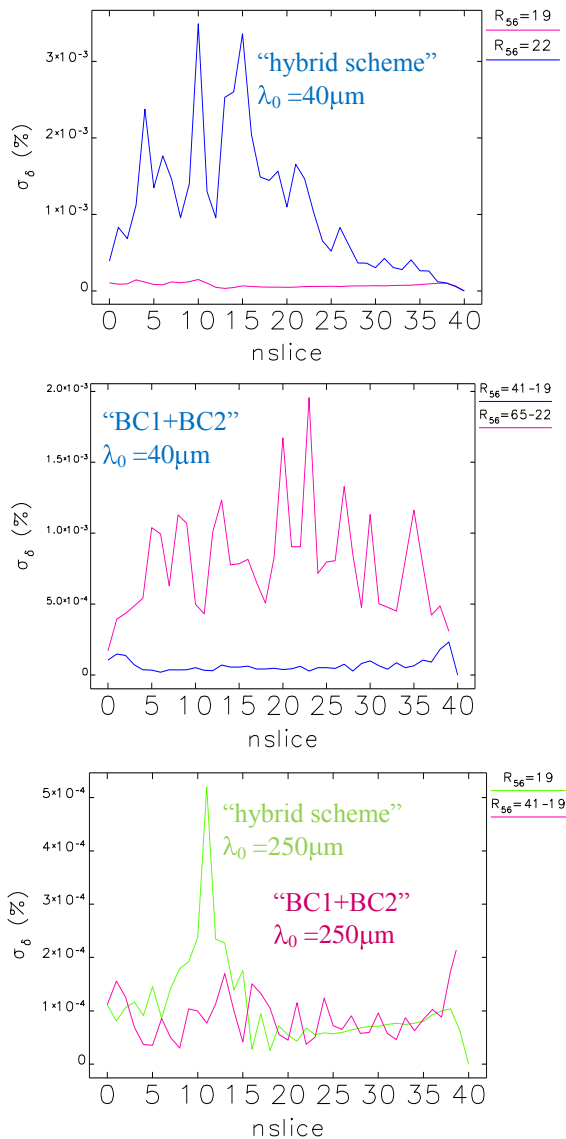


Figure 4-5-6 Slice analysis of the electron beam energy spread at the end of the DL1 dogleg: the “hybrid” compression scheme (top) for  $\lambda_0=40\mu\text{m}$ , the same for the magnetic compression (middle), hybrid and magnetic configuration for  $\lambda_0=250\mu\text{m}$  (bottom). (slice length  $\approx 10 \mu\text{m}$ )

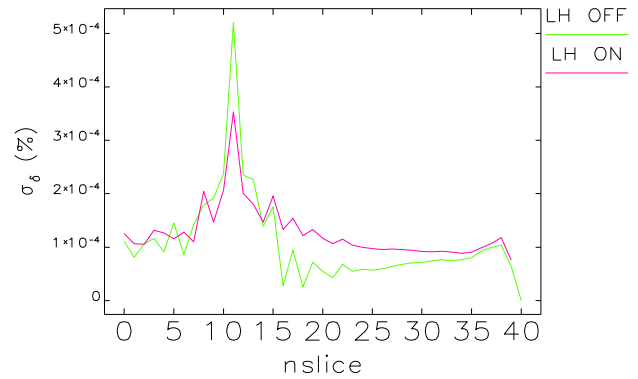


Figure 7: Slice energy spread for the “hybrid” scheme,  $\lambda_0=250\mu\text{m}$ ,

Table 3: Laser Heater Parameter List

electron Energy	160 $\div$ 210 MeV
transv. rms beam size	200 mm
undulator period	0.05 m
undulator parameter	3.00 $\div$ 2.13
undulator length	0.50 m
laser wavelength	800 nm
laser rms spot size	350 mm
laser peak power	1 $\div$ 10 MW

## CONCLUSIONS

Studies of microbunching instability in the SPARX linac have been discussed: two configurations have been considered, the first adopting the “hybrid” compression scheme (velocity bunching + magnetic compressor chicane BC2), the second one using the BC1-BC2 magnetic compressors. According to the theoretical gain curves for the microbunching instability, the accelerator lattice has been optimized in terms of induced slice energy spread of the beam. Further studies are in progress in the modulation wavelength region  $\lambda_0 < 20\mu\text{m}$ , where the purely magnetic compression scheme shows the worse behavior and where a large number of macroparticles is needed to get rid of the simulation numerical noise.

## REFERENCES

- [1] [www.sparx-fel.it](http://www.sparx-fel.it), SPARX-TDR-Team.
- [2] C. Ronsivalle, M. Ferrario, M. Migliorati, C. Vaccarezza, M. Venturini, “Microbunching Studies for SPARX Photoinjector”, this conference
- [3] Z.Huang, *et al.*, PhysRevSTAB.7.074401
- [4] “The SPARC Project”, [www.lnf.infn.it/sparc](http://www.lnf.infn.it/sparc)

## **DISCLAIMER**

This document was prepared as an account of work sponsored by the United States Government. While this document is believed to contain correct information, neither the United States Government nor any agency thereof, nor The Regents of the University of California, nor any of their employees, makes any warranty, express or implied, or assumes any legal responsibility for the accuracy, completeness, or usefulness of any information, apparatus, product, or process disclosed, or represents that its use would not infringe privately owned rights. Reference herein to any specific commercial product, process, or service by its trade name, trademark, manufacturer, or otherwise, does not necessarily constitute or imply its endorsement, recommendation, or favoring by the United States Government or any agency thereof, or The Regents of the University of California. The views and opinions of authors expressed herein do not necessarily state or reflect those of the United States Government or any agency thereof or The Regents of the University of California.